Journal of Organometallic Chemistry 747 (2013) 133–139

Contents lists available at SciVerse ScienceDirect

Journal of Organometallic Chemistry

journal homepage: www.elsevier.com/locate/jorganchem

1,3-Sigmatropic fluorine migration to boron in McLafferty type of rearrangements: Observation of tetrafluorobenzyne radical cation and trifluorobenzyne cation by CID-mass spectrometry

Nanditha G. Nair [a,b], Jose L. Mendoza-Cortes [b], Ravinder Abrol [b], William A. Goddard III [b], V. Prakash Reddy [a,*]

[a] Department of Chemistry, Missouri University of Science and Technology, Rolla, MO 65409, USA
[b] Department of Chemistry and Chemical Engineering, California Institute of Technology, Pasadena, CA 91125, USA

ARTICLE INFO

Article history:
Received 21 February 2013
Received in revised form
1 June 2013
Accepted 6 June 2013

Keywords:
Boroxine
Benzyne radical cation
Benzyne cation
Sigmatropic rearrangement
DFT calculations

ABSTRACT

The electron-impact mass spectra of the tris(pentafluorophenyl)boroxine (**1**) and triphenylboroxine (**2**) were analyzed to probe the McLafferty type of rearrangements involving 1,3-fluorine or 1,3-hydrogen migrations to boron from the adjacent aromatic rings. 1,3-Sigmatropic fluorine migration leading to the McLafferty rearrangement of **1** results in the formation of the tetrafluorobenzyne radical cation (**1c**), whereas the similar rearrangement involving 1,3-hydrogen rearrangement is not observed for the nonfluorinated analog **2**. The DFT calculations show that the activation barrier for the 1,3-fluorine migration in **1** is significantly lower than that for the 1,3-hydrogen migration in **2** ($\Delta\Delta G^{\ddagger}$ ~33 kcal/mol), which is in accordance with the observed 1,3-fluorine migration for the fluorinated boroxine and the lack of such rearrangement for the nonfluorinated boroxine. The 1:1 stoichiometry of the fluoride anion with **1** has also been demonstrated by high resolution electrospray ionization time-of-flight mass spectrometry.

1. Introduction

Selective complexation of fluoride anion makes it possible to use otherwise insoluble LiF as a light weight, high charge density electrolyte in rechargeable lithium ion batteries. Boron based Lewis acid anion receptors for the specific binding to fluoride anion are of enormous interest to the design of lithium ion batteries [1]. For example, pentafluorophenylboron oxalate dramatically increases the solubility of lithium fluoride, lithium oxide and lithium peroxide in carbonate based electrolyte solvents [2,3]. We have earlier reported the fluorinated boroxine, tris(pentafluorophenyl) boroxine (**1**), and other boroxine derivatives as efficient fluoride anion receptors [4]. Using ^{19}F NMR, UV–visible studies and DFT studies, we have investigated the fluoride ion binding abilities of various boroxine derivatives.

The fluoride anion binding affinity increases with increase in the number of the fluorine atoms in the triarylboroxines [4]. Electrospray ionization mass spectrometry (ESI-MS) is a convenient and reliable technique for the investigation of the stoichiometry of the host–guest complexes. We have therefore set out to investigate the fluoride anion complex of **1** by ESI-MS to confirm its fluoride binding stoichiometry. Indeed, as expected from our earlier studies, it shows a 1:1 complex with the fluoride anions (*vide infra*).

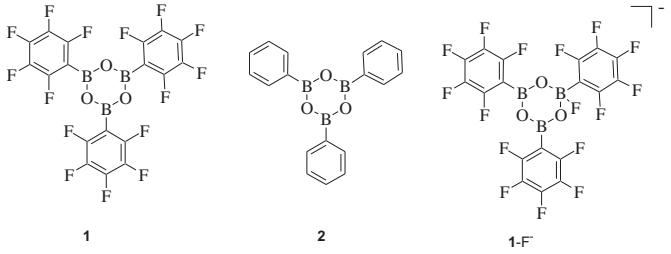

Tandem mass spectrometric techniques also provide an opportunity to investigate the occurrence of the 1,3-fluorine migration during the fragmentation of boroxines [5–8]. Such 1,3-fluorine migrations or 1,3-hydrogen migration during these fragmentation are expected to give the otherwise highly unstable benzyne radical cations, and benzyne cations. There are only few reports on the studies of the benzyne radical cations, and benzyne cation has

* Corresponding author. Tel.: +1 573 341 4768.
E-mail address: preddy@mst.edu (V.P. Reddy).

0022-328X/$ – see front matter © 2013 Elsevier B.V. All rights reserved.
http://dx.doi.org/10.1016/j.jorganchem.2013.06.006

never been investigated experimentally to the best of our knowledge [9–14].

Laser vaporization of magnesium-*o*-difluorobenzene complex in argon carrier gas fails to give the expected benzyne radical cation. However, collision-induced dissociation (CID) of the *o*-difluorobenzene-magnesium radical cation complex gives benzyne radical cation, in a mildly energetic collision [10]. Photolysis of mass-selected *o*-difluorobenzene-magnesium radical cation complexes also gives benzyne radical cations at about 2.2 eV [11,12]. The benzyne radical cation dissociates to ethyne and 1,3-butadiyne radical cation as major products, at a threshold voltage of about 4.6 eV (Equation (1)).

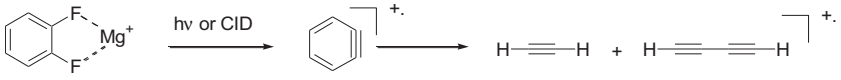

The 1,3-sigmatropic hydrogen or fluorine shift of the boroxines – triphenylboroxine (**2**) and tris(pentafluorophenyl)boroxine (**1**) – are expected to give their corresponding benzyne radical cations. Thus, we have anticipated the ready formation of benzyne radical cations from their precursor boroxines under electron-impact mass spectrometric (EIMS) conditions. Interestingly we find that 1,3-hydrogen shift is disfavored under these conditions and benzyne radical cation is not formed from **2**. On the other hand, tetrafluorobenzyne radical cation **1c** is observed by EIMS of **1** (*vide infra*). We now report the EIMS characterization of the fragmentation products of the boroxines **1** and **2**, and the occurrence of 1,3-sigmatropic fluorine migration for the boroxine radical cation $\mathbf{1}^{+}$. These unexpected results are also corroborated by the DFT calculations.

2. Results and discussion

2.1. Mass spectrometry studies

Electron impact mass spectra (EIMS) for the boroxines **1** and **2** were obtained by a direct insertion probe technique. The compounds were dissolved in dichloromethane and loaded into direct insertion probe on a JEOL JMS-600H double focusing high resolution magnetic sector mass spectrometer. The high resolution MS of **1** shows *m*/*z* 581.988 (calculated mass: 581.9887). High resolution negative ion detected electrospray ionization time-of-flight mass spectrum (ESI-MS/TOF) of a mixture of **1** and KF shows molecular ion peak at *m*/*z* 600.9835 (calculated *m*/*z* 600.9871). The *m*/*z* values for the MF^{-} + 1, MF^{-} − 1, MF^{-} − 2 isotopic peaks are: 601.9943 (calculated *m*/*z* 601.9905), 599.9865 (calculated *m*/*z* 599.9907) and, 598.9968 (calculated *m*/*z* 598.9944), respectively, confirming the 1:1 stoichiometry of the fluoride anion with **1** (Fig. 1). These results are in accordance with expectations based on the ^{19}F NMR, UV–vis titration experiments, and DFT calculations [4].

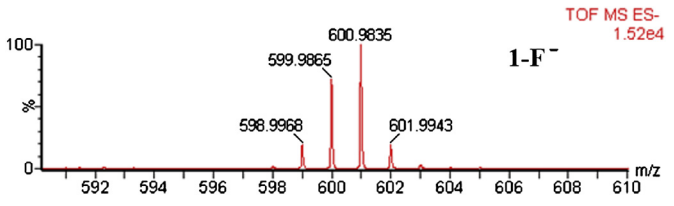

Fig. 1. Negative ion detected high resolution ESI/MS of the fluoride ion complex **1**-F^{-}.

2.1.1. CID/MS studies of boroxines

The collision-induced dissociation mass spectrometry (CID/MS) is ideally suited for the characterization of the fragmentation products of the boroxine radical cations, which may involve benzyne radical cations and benzyne cations. Toward these goals, the abundant molecular ion peaks (*m*/*z* 581.9 and 312.0 for the boroxines **1** and **2**, respectively) were mass-selected and fragmented in a collision cell with xenon gas to obtain the daughter ions. The CID/MS fragmentation of the molecular ion for **1** gave daughter ions at *m*/*z* 433.9, 387.9, 285.9, 193.9, 147.9, 128.9 (Fig. 1). These *m*/*z* values could be readily assigned to fragments **1a**, **1f**, **1b**, **1e**, **1c** and **1d**, respectively, as shown in Scheme 1. On the other hand, the CID/MS of the triphenylboroxine (2; M^{+}; *m*/*z* 312.1) gives fragmentation peaks at *m*/*z* 282.1, 267.1, 235.1, 208.1, 164.1, 131.1, 104, 87, and 77 (Fig. 2). The fragmentation peaks at *m*/*z* 235, 208, 104, and 77 are assigned for the **2a**, **2c**, **2b**, and phenyl radical cation, respectively (Scheme 2) [15,16].

McLafferty rearrangement of the fluorinated boroxine radical cation $\mathbf{1}^{+\bullet}$ (*m*/*z* 581.9) involving 1,3-sigmatropic fluorine shift of the *ortho*-fluorine, followed by concerted cleavage of the boron aryl bond, results in the formation of the tetrafluorobenzyne radical cation, **1c** (*m*/*z* 147.9). The latter tetrafluorobenzyne radical cation **1c** further undergoes cleavage of the adjacent C–F bond to give the highly strained trifluorobenzyne cation (**1d**), at *m*/*z* 128.9. Interestingly, the benzyne cation or any of its derivatives has not been reported to date. The consecutive McLafferty type of fragmentation of **1a** involving a second aryl ring leads to the formation of fragment ion **1b**, at *m*/*z* 286. The radical cations **1e** and **1f** at *m*/*z* 193.9 and 387.9, respectively, are formed presumably by the B–O cleavage of the fluorinated boroxine radical cation $\mathbf{1}^{+}$.

2.1.2. CID-MS/MS of tetrafluorobenzyne radical cation

We have used the collision-induced dissociation tandem mass spectrometry (CID MS/MS) to characterize the fragmentation products of the tetrafluorobenzyne radical cation **1c**, and to investigate the possibility of the formation of the trifluorobenzyne cation **1d** through the dissociation of fluorine from **1c**. The CID MS/MS spectrum for the tetrafluorobenzyne radical cation **1c** (*m*/*z* 148) shows peaks at *m*/*z* 129 (radical cation **1d**), 117 (carbocation **4**), 98 (radical cation **5**) (100%), and 79 (carbocation **6**) (Fig. 3). Apparently, the radical cation **1c** does not undergo the concerted fragmentation to give difluoroacetylene and difluoro-1,3-butyne radical cation, as might have been expected from the reported fragmentation pattern for the corresponding nonfluorinated-benzyne radical cation (Equation (1)) [12]; instead, the radical cation **1c** dissociates a fluorine atom to form the trifluorobenzyne cation, **1d** (*m*/*z* 129). Subsequent fragmentation of the benzyne cation **1d** gives, presumably, carbocation **4** (*m*/*z* 117), radical cation **5** (*m*/*z* 98), and carbocation **6** (*m*/*z* 79) (Schemes 1 and 3). These interesting fragmentation patterns of the fluorinated boroxine radical cation $\mathbf{1}^{+\bullet}$ provide ready access to the corresponding fluorinated benzyne radical cation **1c** and fluorinated benzyne cation **1d**, for further characterization of their thermochemical properties.

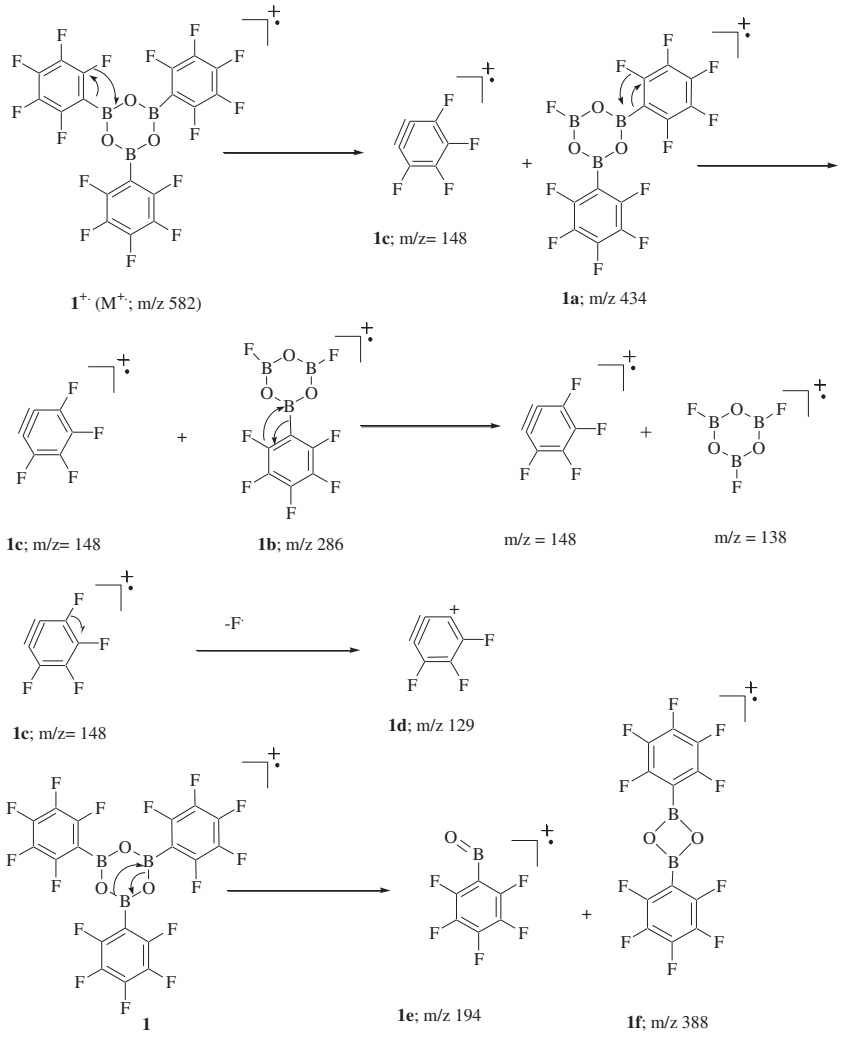

Scheme 1. Proposed fragmentation mechanism of the radical cation $\mathbf{1}^{+}$.

2.2. Theoretical studies

2.2.1. 1,3-Sigmatropic rearrangements

The fragmentation pattern of the EI-HRMS/MS of tris(pentafluorophenyl)boroxine (**1**) reveals the involvement of a 1,3-sigmatropic migration of the *ortho*-fluorine from the aryl rings to boron in concert with elimination of fluorobenzyne (Scheme 1). Such 1,3-fluorine migrations to boron have not been reported to date to the best of our knowledge, although several such 1,3-sigmatropic shifts have been observed for the allyl fluorides [17–19]. The 1,3-sigmatropic fluorine shifts to silicon have also been reported in the 2-phospha-1,3-disilaallyl fluorides ($Bu^t(R)Si{=}P{-}Si(R)Bu^tF$) [20]. Recent DFT theoretical studies indicate that this allowed suprafacial rearrangement proceeds with a four membered C_s transition state in which migrating fluorine has a charge of −0.6e [21].

The 1,3-sigmatropic fluorine migrations to boron have never been reported to the best of our knowledge. In order to probe the nature of the 1,3-sigmatropic shift of fluorine to boron we have calculated the transition structure for this sigmatropic shift (TS 7) and compared it with that of the 1,3-hydrogen shift (TS 8) using DFT calculations. We used B3LYP [22,23] and M06 [24] hybrid DFT functionals as implemented in the Jaguar code [25] with the 6-31G**++ basis set for the structural optimization and 6-311G**++ basis set for single point energy calculations (denoted as B3LYP/6-311G**++//B3LYP/6-31G** and MO6/6-311G**++//MO6/6-31G**, respectively). All geometries were optimized using the analytic Hessian to determine that the local minima have no negative curvatures (imaginary frequencies). The vibrational frequencies from the analytic Hessian were used to calculate the zero-point energy corrections at 0 K (Table 1).

The free energies of activation for the 1,3-fluorine- and 1,3-hydrogen migration reactions, calculated at MO6 and B3LYP levels, are comparable (Table 2). However, the enthalpies of reaction and free energies of reaction obtained at these two levels deviate by about 3 kcal/mol from each other (Table 2). These unattainably high activation barriers (>106 kcal/mol) and high endothermicities (>30 kcal/mol), however, are expected to be significantly reduced in the case of the reactions proceeding from their corresponding boroxine-radical cations. The activation barrier ($\Delta G^{\ddagger}$) for the 1,3-hydrogen migration of the triphenylboroxine **2** is significantly higher than the $\Delta G^{\ddagger}$ for the 1,3-fluorine migration in tris(pentafluorophenyl)boroxine **1** ($\Delta\Delta G^{\ddagger}$ ~33 kcal/mol), which is in accordance with the lack of the 1,3-hydrogen migration for the triphenylboroxine **2** in its EIMS.

The results obtained from B3LYP and M06 calculations, as summarized in Fig. 4, are very similar. However, the ΔG_{rxn} and ΔH_{rxn} of these reactions are, in general, 3 kcal/mol higher at the

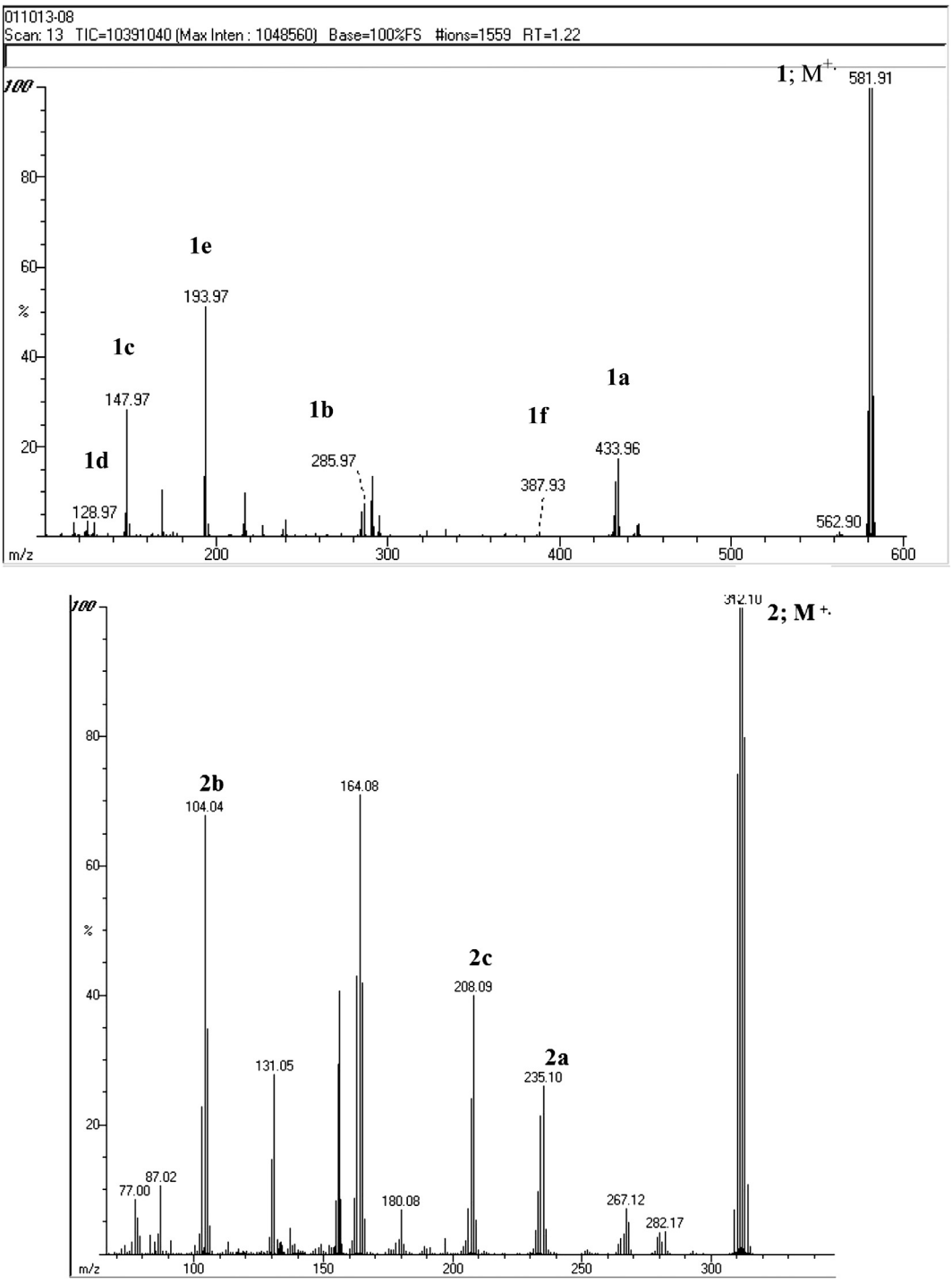

Fig. 2. EI-MS of tris(pentafluorophenyl)boroxine (**1**; top) and triphenylboroxine (**2**; bottom).

M06 level, which was designed to take into account the van der Waals forces. This suggests that the dispersion forces may only play a minor role on the energetics of these reactions. The activation free energies obtained at both of these levels are also very similar.

B3LYP as well as M06 functionals predict that the reactions are highly unfavorable: the products of these McLafferty-type of reactions involving 1,3-fluorine- and 1,3-hydrogen migration are 30 kcal/mol and 83 kcal/mol uphill, respectively. However, although both of these reactions are highly endothermic, the 1,3-fluorine-McLafferty rearrangement is 50 kcal/mol relatively is less endothermic. The calculated transition structures (Fig. 5) have a single negative eigen value and the negative imaginary frequency corresponds to the migrating fluorine and hydrogen bonds. These transition structures show that the 1,3-migration of fluorine or hydrogen is in concert with the carbon–boron bond cleavage. Although the free energies of activation ($\Delta G^{\ddagger}$) for these reactions are unattainable for the neutral compounds under normal conditions, the $\Delta G^{\ddagger}$ calculated for the 1,3-fluorine migration is relatively much lower compared to that of 1,3-hydride migration ($\Delta\Delta G^{\ddagger}$ ~33 kcal/mol) in accordance with the relatively higher affinity of

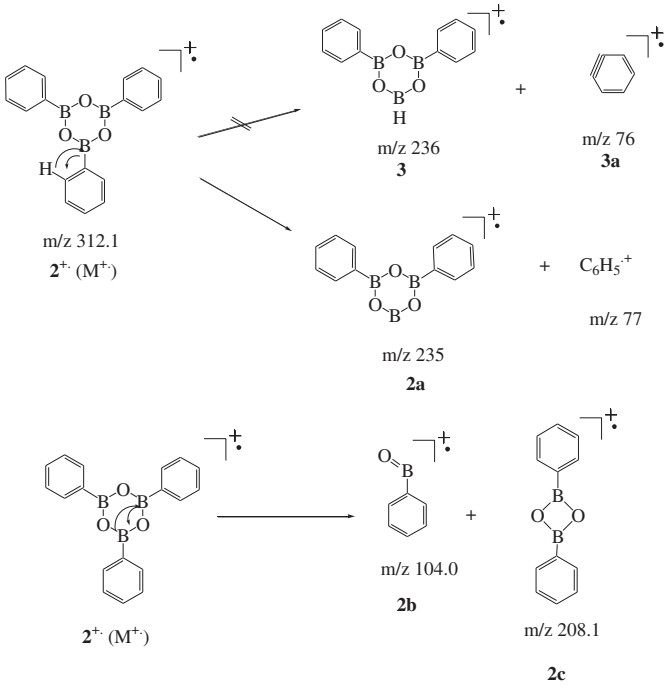

Scheme 2. Proposed fragmentation mechanism for the radical cation $\mathbf{2}^{+\cdot}$.

boron to fluorine as compared to hydrogen. Interestingly, the bond-distances for the dissociating B–C bonds are very similar in the transition structures 7 and 8; 2.45 Å (structure 7; Fig. 5) vs 2.37 Å (structure 8; Fig. 5), showing the similarity of these rearrangements.

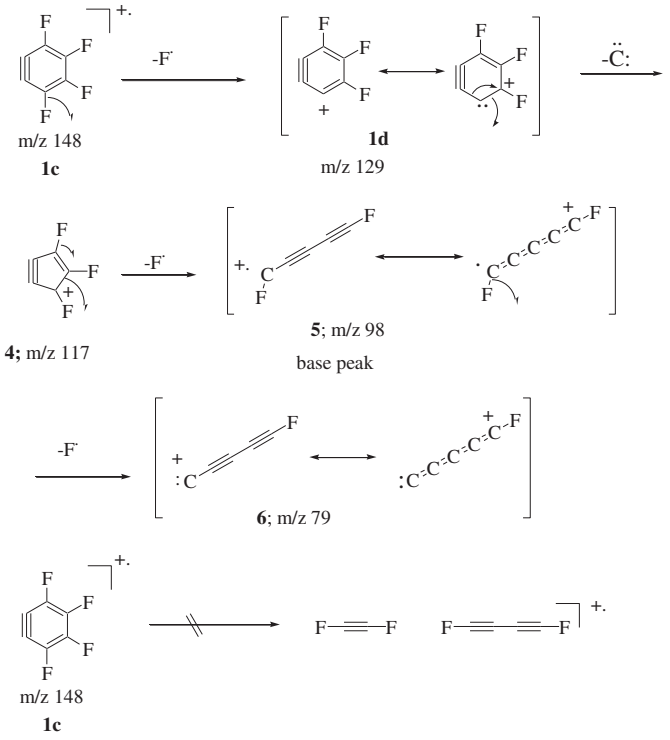

Scheme 3. Proposed mechanism for the fragmentation of the tetrafluorobenzyne radical cation (**1c**; *m*/*z* 148).

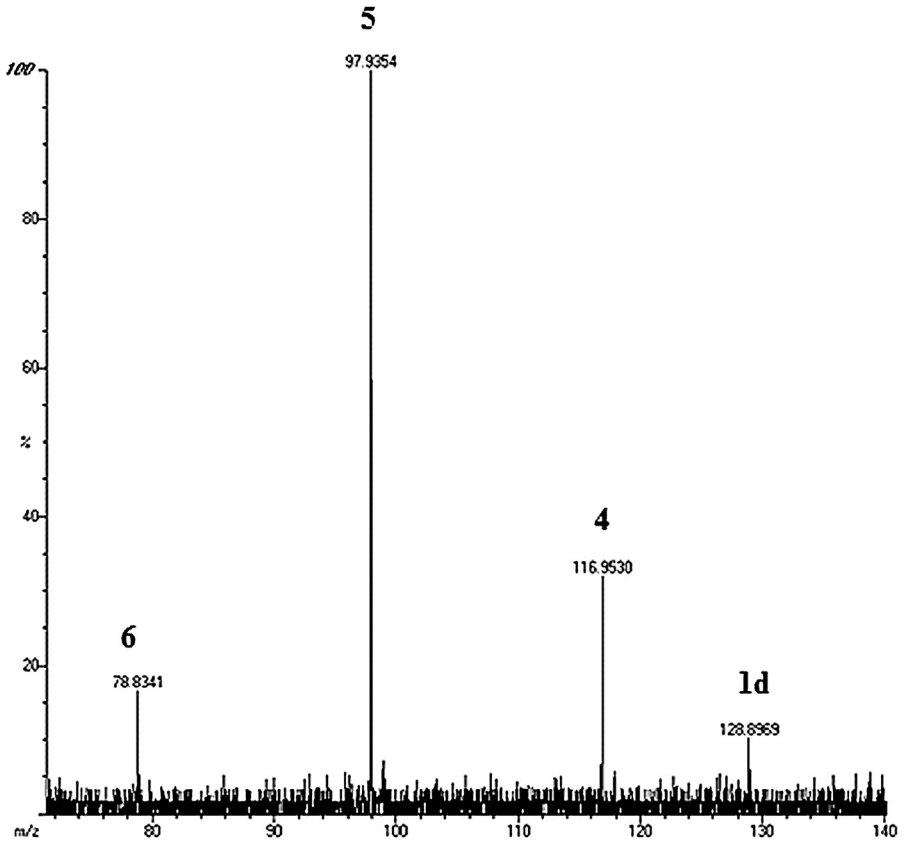

Fig. 3. CID-MS/MS of tetrafluorobenzyne radical cation (**1c**, *m*/*z* 148) showing the formation of the trifluorobenzyne cation (**1d**; *m*/*z* 129) and its subsequent fragment ions.

Table 1
B3LYP/6-311G**++//B3LYP/6-31G** and MO6/6-311G**++//MO6/6-31G** optimized electronic energies (E_{SCF}), zero point energies (ZPE), vibrational enthalpies (H_{vib}), total enthalpies (H_{tot}), vibrational entropies (S_{vib}) and total entropies (S_{tot}) for selected compounds at 298.15 K (‡symbolizes the transition state). All units are in kcal/mol.

Compound	M06	B3LYP	M06	B3LYP	M06		B3LYP		M06		B3LYP	
	E_{SCF}	E_{SCF}	ZPE	ZPE	H_{vib}	H_{tot}	H_{vib}	H_{tot}	S_{vib}	S_{tot}	S_{vib}	S_{tot}
$B_3O_3(PhF_5)_3$	−1.56E+06	−1.56E+06	114.4	112.5	16.1	18.4	17.2	19.6	102.0	182.0	110.2	190.2
$B_3O_3(PhF_5)_2F$	−1.16E+06	−1.16E+06	84.3	82.9	12.4	14.7	12.3	14.7	81.5	162.3	77.6	158.3
PhF_4	−3.94E+05	−3.94E+05	27.6	27.3	3.2	5.5	3.1	5.5	17.2	87.5	17.0	87.3
$B_3O_3(PhF_5)_3^{\ddagger}$	−1.56E+06	−1.56E+06	111.8	109.9	15.1	17.4	17.3	19.7	90.8	174.5	113.8	197.5
$B_3O_3(PhH_5)_3$	−6.24E+05	−6.25E+05	189.1	189.6	10.4	12.8	10.3	12.7	72.5	147.7	71.1	146.3
$B_3O_3(PhH_5)_2H$	−4.80E+05	−4.80E+05	137.9	138.1	7.3	9.7	7.2	9.6	48.4	124.2	47.7	123.6
PhH_4	−1.45E+05	−1.45E+05	46.8	47.2	1.1	3.5	1.0	3.4	5.3	69.6	4.8	69.0
$B_3O_3(PhH_5)_3^{\ddagger}$	−6.24E+05	−6.25E+05	184.9	185.2	9.9	12.2	9.8	12.2	67.0	145.9	66.3	145.2

Table 2
Free energies of reaction (ΔG_{rxn}), enthalpies of reaction (ΔH_{rxn}), and free energies of activation ($\Delta G^{\ddagger}$) for the McLafferty-type of reactions of the fluorinated and nonfluorinated triarylboroxines (**1** and **2**); units are in kcal/mol.

Reaction	M06	B3LYP	M06		B3LYP	
	$\Delta G^{\ddagger}$	$\Delta G^{\ddagger}$	ΔG_{rxn}	ΔH_{rxn}	ΔG_{rxn}	ΔH_{rxn}
$B_3O_3(PhF_5)_3 \rightarrow B_3O_3(PhF_5)_2F + PhF_4$	106.2	101.7	30.4	50.5	30.5	47.0
$B_3O_3(PhH_5)_3 \rightarrow B_3O_3(PhH_5)_2H + PhH_4$	138.7	140.5	83.0	96.7	80.2	94.0

It is evident from the above DFT calculations that the 1,3-shift of fluorine to the electrophilic boron is relatively much faster than that of the 1,3-hydrogen shift, as anticipated for the high fluorophilicity of the boron. The relatively much higher activation barrier for the 1,3-hydrogen migration as compared to the 1,3-fluorine migration is reflected in the observation of the tetrafluorobenzyne radical cation (**1c**) from the corresponding boroxine **1** and the lack of such rearrangement in the triphenylboroxine **2**. Although these calculations reveal unattainably high activation barriers for the neutral boroxines under normal conditions, these barriers are expected to be much smaller for the radical cations or anions that are produced in the mass spectrometers.

2.2.2. Isodesmic calculations

We were intrigued by the absence of 1,3-hydrogen shifts in case of triphenylboroxine radical cation ($\mathbf{2}^{+\cdot}$) and therefore performed DFT calculations for the isodesmic reactions [26] involving benzyne radical cations, **1c** and **3a** (Scheme 4). The open shell UB3LYP/6-311++G** calculations for the latter isodesmic reaction show that the benzyne radical cation is favored with respect to the corresponding trifluorobenzyne radical cation by 9.94 kcal/mol. Thus, based on the thermodynamic grounds, the 1,3-hydrogen migration leading to the McLafferty rearrangement should be favored over that of the 1,3-fluorine migration, which is contrary to our EIMS observations. However, as shown above, the DFT-derived activation barrier for the 1,3-fluorine migration is significantly smaller than that of the 1,3-hydrogen migration by about 33 kcal/mol; there is, therefore, a kinetic preference for the fragmentation of the fluorinated boroxine radical cation ($\mathbf{1}^{+\cdot}$) to give the tetrafluorobenzyne radical cation (**1c**), in spite of its relatively lower thermodynamic stability.

3. Conclusions

Through combined mass spectrometry and DFT calculations of a fluorinated triarylboroxine, we have demonstrated the 1,3-sigmatropic migration of fluorine to boron leading to the McLafferty type of fragmentation. The calculated activation barrier for the 1,3-fluorine migration in the tris(pentafluorophenyl)boroxine **1** is significantly lower (by ~33 kcal/mol) than that of the 1,3-hydrogen migration for the corresponding nonfluorinated boroxine **2**, in accordance with our experimental observations. The mass spectrometric fragmentation of the boroxine **1** provides a convenient access to the tetrafluorobenzyne radical cation **1c**, and a hitherto

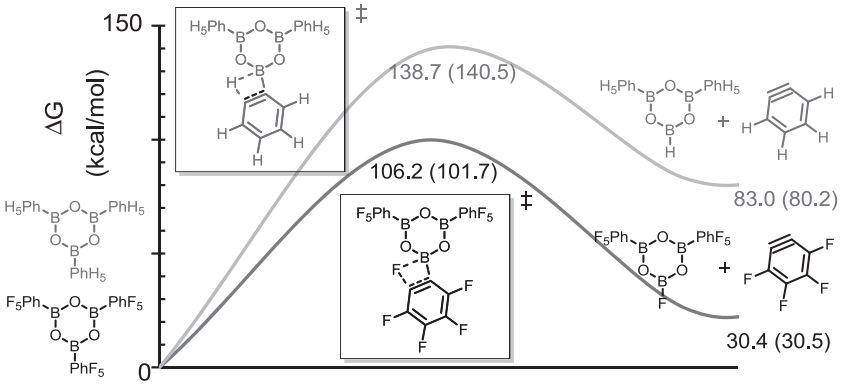

Fig. 4. M06/6-311G**++//M06/6-31G** (and B3LYP/6-311G**++//B3LYP/6-31G**, in parentheses) derived free energies of activation and free energies of reaction for the McLafferty-type of rearrangements involving sigmatropic 1,3-fluorine and 1,3-hydrogen migrations.

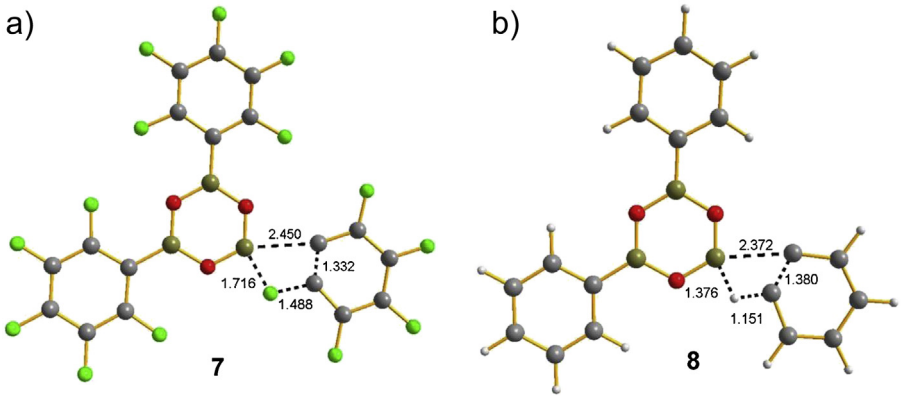

Fig. 5. Transition structures (selected bond distances in Å) for a) 1,3-fluorine- and b) 1,3-hydrogen migration for **1** and **2**, at M06/6-31G** level of DFT calculations.

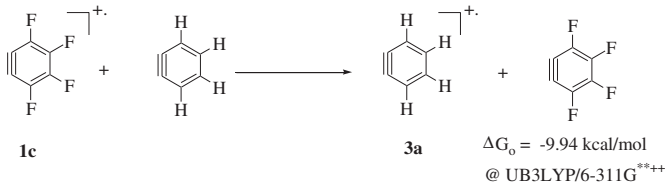

Scheme 4. Isodesmic reaction for comparing the relative stabilities of benzyne radical cation and tetrafluorobenzyne radical cation (**1c**).

unreported trifluorobenzyne cation **1d**. The 1:1 stoichiometry of the fluoride anion with boroxine **1** has also been demonstrated by high resolution electrospray ionization time-of-flight mass spectrometry. Further experimental and theoretical studies are in progress in our laboratories to elucidate the structural and mechanistic details of these unique high energy species.

4. Experimental section

4.1. Mass spectroscopic studies

Boroxines **1** and **2** are synthesized as reported earlier by dehydrative-cyclization of the corresponding boronic acids [4]. The sample for mass spectroscopic analysis was prepared in anhydrous dichloromethane solution (0.05 mg/mL) for high resolution ESI-MS/TOF and EIMS. The sample for ESI-HRMS was prepared by dissolving 1:1 M ratio of tris(pentafluorophenylphenyl)boroxine (**1**) and potassium fluoride (KF) in dichloromethane solution. The sample was analyzed by electrospray ionization (ESI) in the negative ion mode using an LCT Premier XE time-of-flight (TOF) mass spectrometer (Waters) that was operated in the W mode resulting in resolution of ~10,000. For these experiments, the capillary voltage was set at −3500 V, sample cone at 45 V, desolation temperature 250 °C, and source temperature 120 °C. The cone gas flow was 10 and the desolvation flow was 600 (arbitrary units for the instrument). The sample was infused at ~50 uL/minute.

The EIMS were obtained by electron impact ionization (70 eV electron beam) using a heated direct insertion probe on a JEOL JMS-600H double focusing high resolution magnetic sector mass spectrometer. For the tandem mass spectrometric experiments, the precursor ions were selected and fragmented in a collision cell with Xe gas.

4.2. Theoretical studies

The DFT calculations were carried out using B3LYP [22,23] and M06 [24] hybrid DFT functionals as implemented in the Jaguar code [25] with the basis sets 6-31G**++ for optimization and 6-311G**++ for single point energies.

Acknowledgments

We gratefully acknowledge Mona Shahgholi at Caltech mass spectroscopic facilities for EI/HRMS spectra. One of us (NN) thanks Dr. Simon Jones and Professor Robert H. Grubbs for their encouragement.

References

[1] X. Sun, H.S. Lee, X.Q. Yang, J. McBreen, Electrochem. Solid-State Lett. 5 (2002) A248–A251.
[2] Z. Chen, K. Amine, J. Electrochem. Soc. 156 (2009) A672–A676.
[3] B. Xie, H.S. Lee, H. Li, X.Q. Yang, J. McBreen, L.Q. Chen, Electrochem. Commun. 10 (2008) 1195–1197.
[4] N.G. Nair, M. Blanco, W. West, F.C. Weise, S. Greenbaum, V.P. Reddy, J. Phys. Chem. A 113 (2009) 5918–5926.
[5] J.P. Da Silva, R. Kulasekharan, C. Cordeiro, S. Jockusch, N.J. Turro, V. Ramamurthy, Org. Lett. 14 (2012) 560–563.
[6] Y. Ma, X. Ji, F. Xiang, X. Chi, C. Han, J. He, Z. Abliz, W. Chen, F. Huang, Chem. Commun. 47 (2011) 12340–12342.
[7] M.H. Mohamed, L.D. Wilson, J.V. Headley, K.M. Peru, Rapid Commun. Mass Spectrom. 23 (2009) 3703–3712.
[8] H.F. Nour, T. Islam, M. Fernandez-Lahore, N. Kuhnert, Rapid Commun. Mass Spectrom. 26 (2012) 2865–2876.
[9] H. Li, M.-B. Huang, Phys. Chem. Chem. Phys. 10 (2008) 5381–5387.
[10] H. Liu, S. Yang, I. Balteanu, O.P. Balaj, B.S. Fox-Beyer, M.K. Beyer, V.E. Bondybey, Rapid Commun. Mass Spectrom. 18 (2004) 1479–1481.
[11] H. Liu, X. Zhang, C. Wang, W. Guo, Y. Wu, S. Yang, J. Phys. Chem. A 108 (2004) 3356–3366.
[12] H.-C. Liu, C.-S. Wang, W. Guo, Y.-D. Wu, S. Yang, J. Am. Chem. Soc. 124 (2002) 3794–3798.
[13] H.-C. Liu, X.-H. Zhang, Y.-D. Wu, S. Yang, Phys. Chem. Chem. Phys. 7 (2005) 826–831.
[14] B.F. Yates, Int. J. Mass Spectrom. 201 (2000) 297–305.
[15] C.J.W. Brooks, D.J. Harvey, B.S. Middleditch, Org. Mass Spectrom. 3 (1970) 231–235.
[16] R.H. Cragg, J.F.J. Todd, A.F. Weston, Org. Mass Spectrom. 6 (1972) 1077–1081.
[17] M.G. Barlow, R.N. Haszeldine, C.J. Peck, J. Fluorine Chem. 18 (1981) 601–604.
[18] M.G. Barlow, R.N. Haszeldine, C.J. Peck, J. Fluorine Chem. 20 (1982) 771–776.
[19] J. Burdon, A. Childs, I.W. Parsons, T.W. Rimmington, J. Fluorine Chem. 18 (1981) 75–85.
[20] M. Driess, S. Rell, H. Pritzkow, R. Janoschek, Angew. Chem. Int. Ed. Engl. 36 (1997) 1326–1329.
[21] E. Chamorro, J.C. Santos, B. Gomez, R. Contreras, P. Fuentealba, J. Chem. Phys. 114 (2001) 23–34.
[22] A.D. Becke, J. Chem. Phys. 98 (1993) 5648–5652.
[23] C.T. Lee, W.T. Yang, R.G. Parr, Phys. Rev. B 37 (1988) 785–789.
[24] Y. Zhao, D.G. Truhlar, Acc. Chem. Res. 41 (2008) 157–167.
[25] R.D. Chambers, J. Fluorine Chem. 131 (2010) 665–675.
[26] S.E. Wheeler, K.N. Houk, P. v. R. Schleyer, W.D. Allen, J. Am. Chem. Soc. 131 (2009) 2547–2560.